HEAT TRANSFER IN A ROTARY KILN DURING DRYING AND PREHEATING OF WET SOLIDS

A Thesis Submitted
In Partial Fulfilment of the Requirements
for the Degree of

MASTER OF TECHNOLOGY

by

ANANDAN UNNI. V. K.

to the

DEPARTMENT OF MECHANICAL ENGINEERING

INDIAN INSTITUTE OF TECHNOLOGY, KANPUR

JULY, 1988

Certificate

This is to certify that the work on "HEAT TRANSFER IN A ROTARY KILN DURING DRYING AND PREHEATING OF WET SOLIDS" has been carried out under my supervision and has not been submitted elsewhere for a degree.

July, 1988.

(P.S. Ghoshdastidar)
Assistant Professor
Department of Mechanical Engineeri
Indian Institute of Technology
Kanpur-208016

ACKNOWLEDGEMENTS

I would like to express my sincere gratitude to Dr. P.S. Ghoshdastidar for his guidance and critical appraisal throughout the course of the present work.

I am also thankful to Sri U.S. Misra who did an excellent job in typing this thesis and to Sri J.C. Verma who did a neat work of all the drawings.

-V.K. Anandan Unni

CONTENTS

LIST OF TABLES

LIST OF FIGURES

NOMENCLATURE

a	Thermal diffusivity of refractory
A	Area
C	Specific heat of refractory
C_p	Specific heat of gas/solid
D	Diameter of the kiln
h_r	Radiation heat transfer coefficient
h_c	Convection heat transfer coefficient from outer wall
h_{cs}	Heat transfer coefficient from the refractory to solid
K	Thermal conductivity of the refractory
$\dot{m}$	Mass flow rate
N	Number of elements of the wall and the solid
q	Heat transfer rate
R	Radius of the kiln
S	Rotational speed of the kiln
T	Temperature (^{o}K)
U	Circumferential velocity of the kiln wall
X	Coordinate in the radial direction
ΔX	Grid size in the X-direction
Y	Coordinate in the circumferential direction
ΔY	Grid size in the Y-direction
ΔZ	Size of each segment in the axial direction

Greek Letters

α	Fill angle
σ	Stefan - Boltzman constant
ε	Emissivity
ρ	Density
Θ	As defined in Fig. 2(a)
$\Delta\tau$	Time step.

Subscript

g	Gas
i	Element number of the wall or the solid
j	Element number of the wall or the solid
l	Liquid
m	Grid number in X-direction
n	Grid number in Y-direction
rf	Refractory
s	Solid
V	Vapour
Z	Axial direction

Superscripts

p	Present
p+1	Future.

ABSTRACT

In the present study, a rigorous heat transfer model has been developed for a rotary kiln used for drying and preheating of wet solids. The results have been checked by applying this model to the non-reacting zone of a cement rotary kiln mentioned in a previous work .

A rotary kiln consists of a refractory lined cylindrical shell mounted at a slight incline from the horizontal plane. The kiln is very slowly rotated about its longitudinal axis. The wet solid is fed into the upper end of the cylinder and during the process is dried and preheated by the counter-current flow of the hot gas. Finally, it is transferred to the lower end where it is discharged.

In the present work, a heat transfer model is developed which includes radiation from the hot gas and transient conduction in the wall and mass and energy balances of the hot gas and the solid. The main objectives of this investigation are to determine the length of the kiln required to dry and preheat the wet solids to a desired temperature and also the axial gas and solid temperature distribution.

To compute the radiation heat transfer, the wall and the solid surface are divided into twenty elements that

form a gray enclosure. Hot gas which emits, absorbs and transmits radiation fills the enclosure. The shape factors between the elements are determined and the net radiation exchanged is computed using gas-radiation theory. Heat conduction in the refractory wall is determined using the finite difference technique and assuming heat conduction only in the radial direction. Convection heat transport due to kiln rotation is included in the energy balance of the wall elements. The rate of vaporisation of the wet solids is determined by making a mass and energy balance of the solids.

Although the results show that the predicted length is much lower than that of the actual kiln, the axial solid and gas temperature distribution Vs. percent kiln length matches well with the actual kiln profile. It is also seen that there is virtually no circumferential variation of refractory wall temperature. The radial wall temperature variation is seen to be almost linear.

Chapter 1

1.1 Introduction

Although rotary kilns are used in many chemical and metallurgical industries, the information that have been published regarding the heat transfer analysis and design of these units are very few. In the present study, a heat transfer model is developed for the non-reacting zone of a cement rotary kiln. Basically, this model can be used for any rotary kiln which is used for drying and preheating of wet solid, e.g., preheating of wet iron ore in metallurgical industry.

A rotary kiln consists of a refractory lined cylindrical shell mounted at a slight incline from the horizontal plane. The kiln is very slowly rotated about its longitudinal axis. The solid is fed into the upper end of the cylinder and during the process is transferred towards the lower end where it is discharged. Hot gas is fed into the lower end of the cylinder so that the flow is counter current. Fig. 1 shows the schematic diagram of a rotary kiln.

In the present study, the kiln can be considered to consist of three sections. In the first section, the wet solids are heated to the boiling point of the entrained liquid. In the second region, the liquid

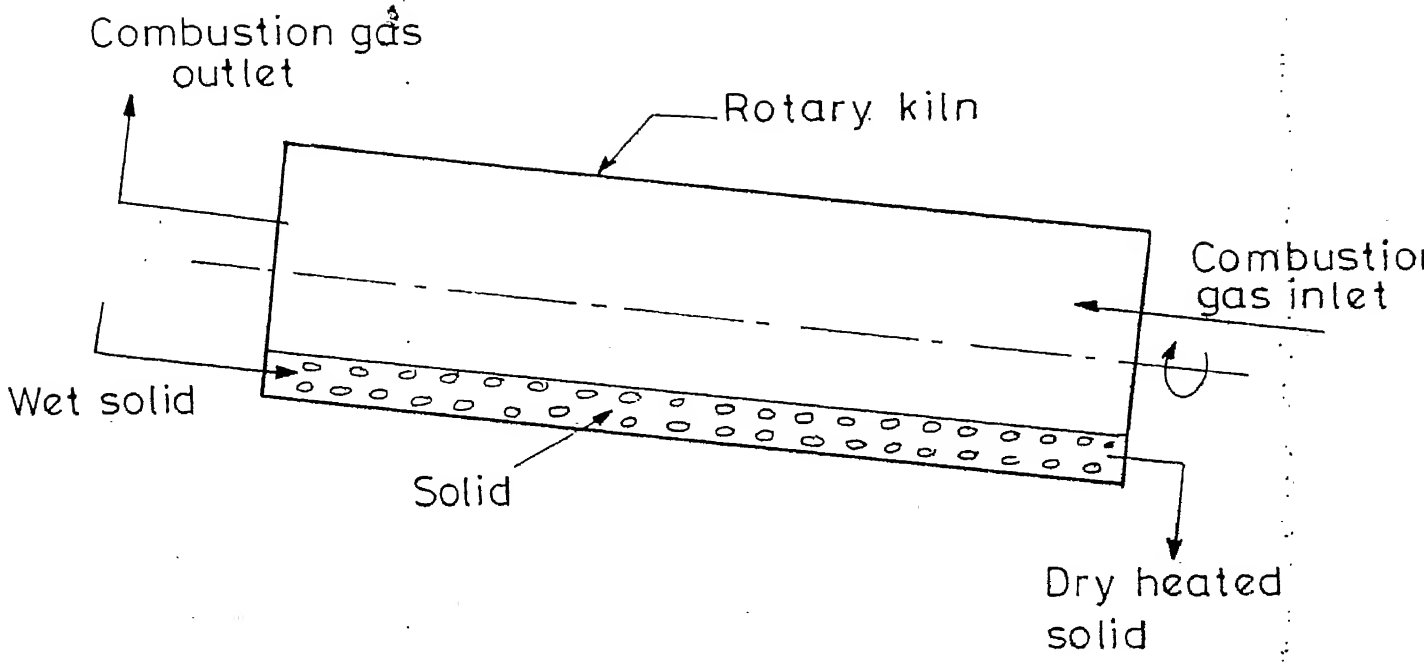

FIG.1 SCHEMATIC DIAGRAM OF A ROTARY KILN

evaporates at constant temperature until the feed is completely dry. In the third region, the solids are heated to some desired temperature and then are discharged from the kiln. The influence of simultaneous mass transfer and chemical reaction has not been considered in this study.

The efficiency of heating in rotary kiln heaters is better because of improved heat transfer to the solids. The rotation of the kiln continuously mixes the solids and therefore, the heat transfer rate is not limited by solid conduction. In addition, the heat is transferred from the refractory wall to the solid in the region of contact. Due to rotation, the refractory wall is alternately heated and cooled by the hot gas and the solid material. Fig. 2(a) shows the nomenclature of the kiln. The angle, α, is called the fill angle which shows the region of volume containing the solid. The angle, θ, is measured from the origin in clockwise direction. The origin is represented by the line joining the center of the kiln and the right extreme point of the solid cross section. The internal radius of the kiln is represented by the symbol, R.

Figure 2(b) shows the heat transfer mechanisms occurring in the kiln. The inner wall which is not covered by the kiln, the solid surface, and the hot gas exchange heat between each other by radiation. The

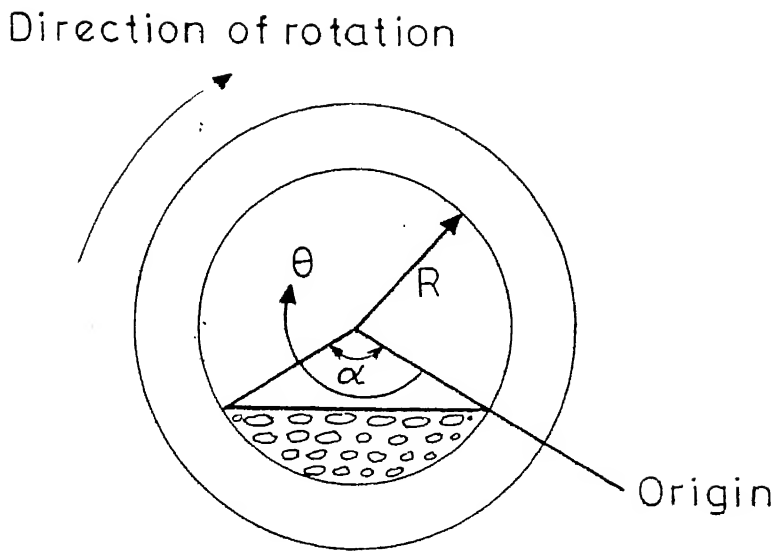

FIG. 2(a) SCHEMATIC CROSS SECTION OF A KILN MODEL

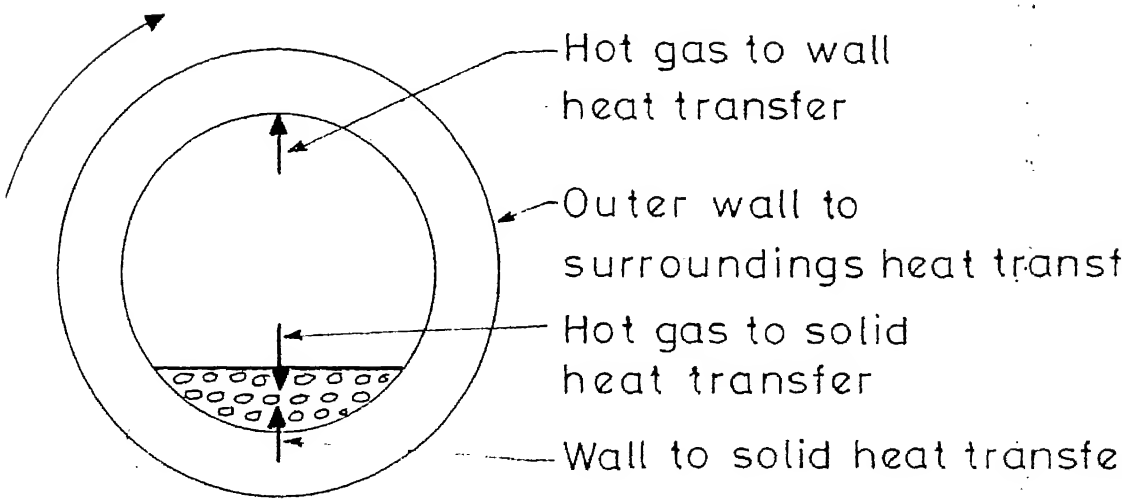

FIG. 2(b) SCHEMATIC DIAGRAM SHOWING HEAT TRANSFER PROCESS IN ROTARY KILN

solid receives heat from the inner wall covered by it. Also, heat is lost from the kiln outer wall to the surroundings.

1.2 Literature Survey

Sass [1] investigated cement kilns and iron ore kilns and Manitius, Kureyusz and Kawecki [2] studied rotary kilns used for the calcination of basic ammonium aluminium sulphate. Sass's work did not consider chemical reactions and mass transfer from solid material but Manitius et.al. included these effects. Mauson, L. and Unger, S. [3] discussed the heat transfer in a rotary kiln incinerator and presented the applicable relations. Recently Ghoshdastidar et al [4] developed a detailed heat transfer model for the rotary kiln waste incinerator. This model included radiation between the flame and refractory surface, transient conduction in the wall and chemical reaction in the waste material. It can predict the length of the kiln required to completely burn plexiglas (Polymethyl-methacrylate) for various fill angles.

1.3 Objectives

The objectives of the present work are:

(i) to develop a rigorous heat transfer model

for rotary kilns used to dry and preheat wet solids, e.g. in cement and metallurgical industries.

(ii) to apply the present model to the rotary cement kiln of Sass [1] and compare the results, i.e. predicted length of the kiln and axial solid and gas temperature variations.

(iii) to check the validity of Sass's assumption that no circumferential temperature variation exists in the kiln.

(iv) to plot the radial temperature distribution in the wall.

Chapter 2

Problem Formulation

2.1 Radiation Heat Transfer between the Hot Gas, the Refractory Wall and the Solid Surface

Heat is exchanged between the hot gas, the inner wall of the kiln and the solid surface by radiation. Since the temperature of the wall varies circumferentially and axially, the wall is divided into surface elements as shown in Fig. 3. The elements that are not covered by the solid and the elements on the surface of the solid are exposed to radiation from the hot gas. The portion on the wall is divided into 15 elements and the solid surface is divided into 5 surface elements. Convection from the gas is neglected as radiation is predominant mode since temperature of the gas is very high.

In this study, for the purpose of calculating emissivity and other characteristics, the composition of hot gas has been taken from Ing. Paul Weber [5], the reason being non-availability of gas composition data for Sass's kiln. The radiation heat transfer among the surface elements of adjoining axial segments is found to be insignificant for the segment length of importance in this study. Therefore, the radiation heat transfer is assumed to occur only among the 20 surface

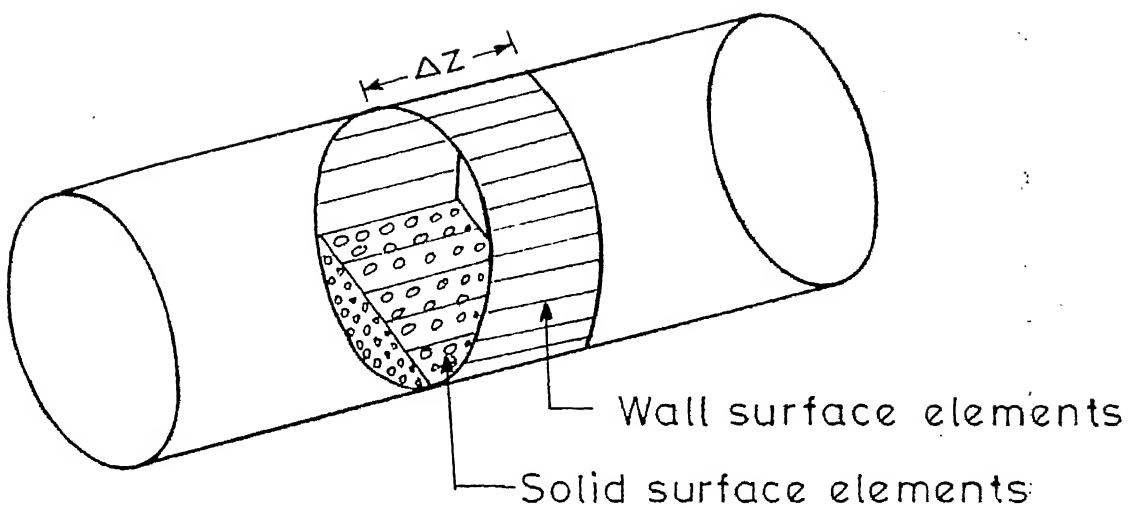

FIG. 3 SECTION OF THE KILN SHOWING SURFACE ELEMENTS OF THE WALL AND THE SOLID

elements in each axial segment.

The radiation heat transfer is calculated by using the theory [6] of gray enclosure containing a gas which emits, absorbs and transmits radiation. Thus, if the gas volume is enclosed by N black surfaces at different temperatures, the net energy gain for a particular surface can be expressed as

$$q_j = G_j A_j - E_{bj} A_j \tag{2.1}$$

where G_j and E_{bj} are irradiation and black body emission per unit area of surface j. Irradiation of surface j = Irradiation from gas + Irradiation from all other surfaces through gas. Or,

$$G_j A_j = A_g F_{gj} \varepsilon_g(T_g) E_{bg} + \sum_{i=1}^{N} A_i F_{ij} \tau_g(T_i) E_{bi} \tag{2.2}$$

where F_{ij} is the shape factor, ε is the emissivity, τ is the transmissivity and E_{bg} and E_{bi} are σT_g^4 and σT_i^4 respectively.

Heat exchange in gray enclosure can be calculated as

$$q_{gray} = q_{black} \cdot \frac{\varepsilon+1}{2} \quad \text{for} \quad \varepsilon > 0.8$$

where ε is the emissivity of wall [6]. In our problem emissivities of refractory and solid are taken as 0.9 and 0.95 respectively.

For the above analysis, shape factors are calculated as shown in Appendix A. Gas emissivity at different gas temperatures are calculated as given in Appendix B. Solving

the above equations (2.1) and (2.2), heat gain/loss of each surface is calculated. The temperature of solid surface elements are taken to be uniform in each axial segment. The refractory wall surface element temperature is determined by radiation input to the surface q_j, heat conduction in the wall and the rotational speed of the kiln using the method outlined in the next section.

2.2 Conduction Heat Transfer in Refractory Wall

Since wall elements of the kiln are alternately heated and cooled during each revolution by the hot gas and the solid respectively, non steady heat conduction is present. Only heat conduction in the radial direction of the wall is taken into account, assuming negligible conduction in the circumferential and axial direction, as the circumference and length of the kiln are much greater than the thickness of the kiln. For a coordinate system that is fixed to rotary kiln, the temperature varies with time and consequently energy storage term is needed in the energy equation. However, for a coordinate system that is stationary, the temperature remains constant and hence the heat storage term is not required. However, the kiln wall now has a velocity with respect to the coordinate system and hence the convective term has to be introduced. Because the nonrotating coordinate system is more conveniently combined with the radiation boundary condition discussed in

the previous section, this coordinate system is chosen for the analysis.

The coordinate system used to model the wall heat conduction is shown in Fig. 4. Because the refractory thickness is small compared to the diameter, cartesian coordinates are used instead of cylindrical coordinates. The X and Y coordinates are in the radial and circumferential directions, respectively. The energy equation for the wall then becomes

$$U \frac{\partial T}{\partial y} = a_{rf} \frac{\partial^2 T}{\partial x^2} \tag{2.3}$$

where U is the circumferential velocity of the wall and a_{rf}, the thermal diffusivity of the refractory. The left hand term of the above equation accounts for the energy convection by the refractory wall and the right hand term is the radial conduction.

The boundary condition for the inner surface of the refractory is dependent upon whether the surface element is exposed to the hot gas or covered with the solid. Elements exposed to gas are heated by radiation and the heat input is q_j, obtained from equation (2.1) in the previous section. Convection heat transfer by the gas is assumed small compared to radiation and therefore is neglected. Surface elements covered by solid exchange heat with solid primarily by surface contact. Helmrich and

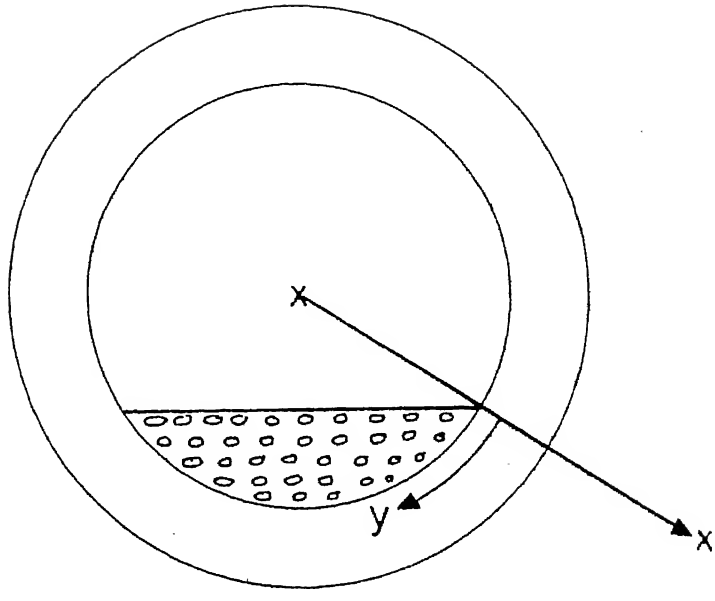

FIG.4 SECTION OF THE KILN SHOWING THE COORDINATE SYSTEM

Schugerl [7] investigated the heat transfer between kiln and the solid over a range of particle diameters. They expressed heat transfer rates as a product of heat transfer coefficient and the difference between the wall and bulk particle temperatures. The same approach is used in the present study. Therefore,

$$q_j = h_{cs} \cdot A_j \, (T_{sj} - T_s) \qquad (2.4)$$

where q_j is the heat transfer rate, h_{cs} is the heat transfer coefficient, A_j is the surface element area, T_{sj} is the refractory wall surface temperature and T_s is the solid temperature. Since the heat transfer coefficient, h_{cs} is not available for the non-reacting part of the cement kiln, in the present study a value of 64 W/m^2-K has been used. This value is for the calcination range of the kiln as given by Helmrich and Schugerl [7].

The boundary condition for the outer surface of the refractory wall is the convection and radiation heat losses. N.V. Suryanarayana et al [8] have investigated the convection and radiation losses from a rotary kiln for various wind velocity, orientation of the kiln, rotational speed of the kiln etc. In the present investigation, convection heat transfer coefficient, h_c is taken as 10 W/m^2-K considering wind is blowing over the

kiln. Radiation heat transfer coefficient is calculated as follows:

$$h_r = \frac{\sigma \varepsilon_{rf} (T_n^4 - T_\infty^4)}{(T_n - T_\infty)}$$

$$\text{i.e.} \quad h_r = \sigma \varepsilon_{rf} (T_n + T_\infty)(T_n^2 + T_\infty^2) \tag{2.5}$$

where T_n and T_∞ are outer wall temperature and ambient temperature respectively.

Then combined heat loss from outer surface is calculated as

$$q_j = (h_c + h_r) A_j (T_j - T_\infty) \tag{2.6}$$

where T_j is the temperature of outer wall element and A_j is the area of that element.

Equation (2.3) is solved numerically by first transforming it into finite difference form. The details of finite difference scheme and its method of solution are given in Appendix C.

In the finite difference scheme, the circumferential elements of the refractory wall are alligned with the wall surface elements as shown in Fig. 3. Five additional elements are taken for the region covered with solid.

Conduction through the wall is simulated by sectioning the wall into ten layers separated by equal gap.

2.3 Energy Transport in Solid

As has been mentioned earlier, the kiln can be considered to consist of three sections, viz., first section in which wet solids are heated to the boiling point of the entrained liquid, second section in which liquid evaporates at constant temperature and the third section in which dry solids are heated to the required temperature.

In the first and third sections, the physical processes are similar, the only difference being, in the first section it is wet solid and in the third section it is dry solid. Fig. 5 shows the energy balance on an element of solid contained in an axial segment either in the first or in the third section of the kiln.

From Fig. 5, it can be seen that

$$\dot{m}_{S.Z}\, C_{ps}\, T_{SZ} + q_1 + q_2 = \dot{m}_{S.Z+\Delta Z}\, C_{ps}\, T_{S.Z+\Delta Z}$$

But since no evaporation takes place, we see that $\dot{m}_{S.Z} = \dot{m}_{S.Z+\Delta Z}$. Then above equation can be written as follows:

$$T_{S.Z+\Delta Z} = T_{S.Z} + \frac{(q_1 + q_2)}{\dot{m}_{S.Z}\, C_{ps}} \qquad (2.7)$$

where q_1 and q_2 are the total radiation heat transfer from the gas and heat transfer from the inner refractory wall to the solid respectively and C_{ps} and $\dot{m}_{S.Z}$ are specific heat and mass flow rate respectively of wet or dry solid as the case may be.

In the second section of the kiln, the evaporation of the entrained liquid takes place and so the solid temperature remains constant at the boiling point of the entrained liquid. Fig. 6 shows the mass balance of solid in the second section. The mass balance equation can be written as

$$\dot{m}_{S.Z+\Delta Z} = \dot{m}_{S.Z} - \dot{m}_V \tag{2.8}$$

where $\dot{m}_V$ is the rate of evaporation in that segment. Fig. 7 shows the energy balance of wet solid in the second section. The energy balance equation can be written as

$$\dot{m}_{S.Z}\, C_{ps}\, T_{S.Z} + q_1 + q_2 = \dot{m}_V\, (L + C_{pl}\, T_{S.Z}) + \dot{m}_{S.Z+\Delta Z}\, C_{ps}\, T_{S.Z} \tag{2.9}$$

Solving equations (2.8) and (2.9), we can see that rate of evaporation $\dot{m}_V$ is obtained as

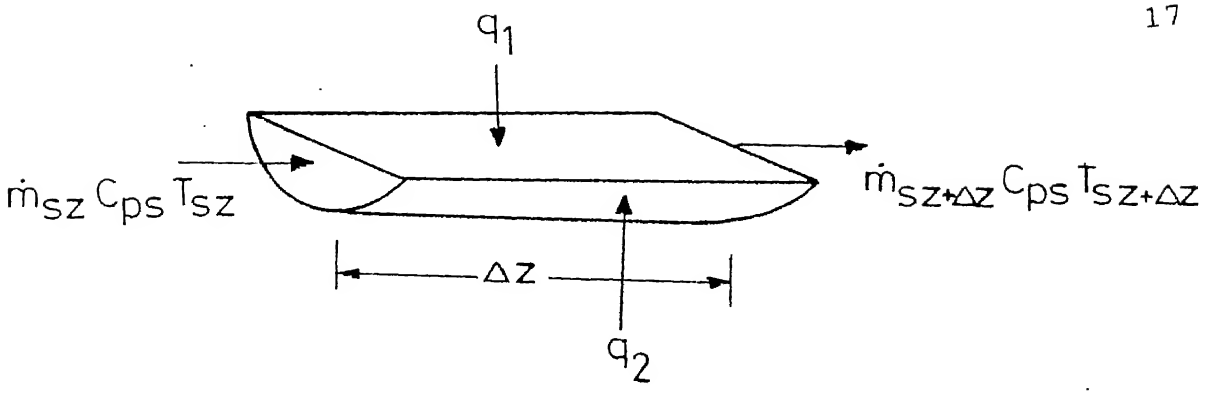

FIG.5 ENERGY BALANCE OF SOLID ELEMENT CONTAINED IN AN AXIAL SEGMENT IN THE 1st OR 3rd SECTION OF THE KILN

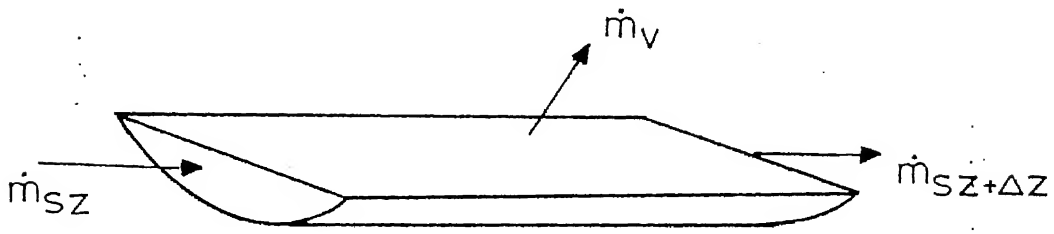

FIG.6 MASS BALANCE OF SOLID IN THE SECOND SECTION OF THE KILN

$$\dot{m}_V = \frac{q_1 + q_2}{L} \tag{2.10}$$

where L is the latent heat of evaporation of the entrained liquid.

Since the first 5 elements are on the surface of the solid, total radiation heat transfer, q_1, is

$$q_1 = \sum_{J=1}^{5} q_j \tag{2.11}$$

where q_j is the same as given in equation (2.1).

Similarly, the heat transfer from the refractory, q_2, is given by

$$q_2 = \sum_{j=1}^{5} h_{cs} A_j (T_{sj} - T_s). \tag{2.12}$$

2.4 Energy Balance in Gas

In the first and third sections of the kiln, only heating of wall surface and solid is taking place. Also, it is to be noted that the flow of gas is in the opposite direction of solid flow. Fig. 8 shows the energy balance of hot gas in the first and third sections.

We can write the energy balance equation as

$$\dot{m}_{g.Z+\Delta Z} \; C_{pg} \; T_{g.Z+\Delta Z} = \dot{m}_{g.Z} \; C_{pg} \; T_{g.Z} + q_r \tag{2.13}$$

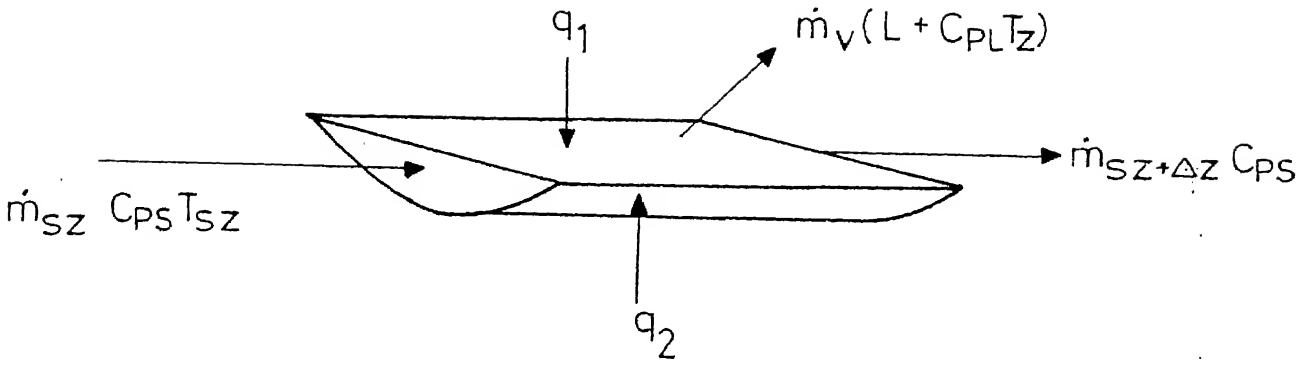

FIG.7 ENERGY BALANCE OF SOLID IN THE SECOND SECTION OF THE KILN

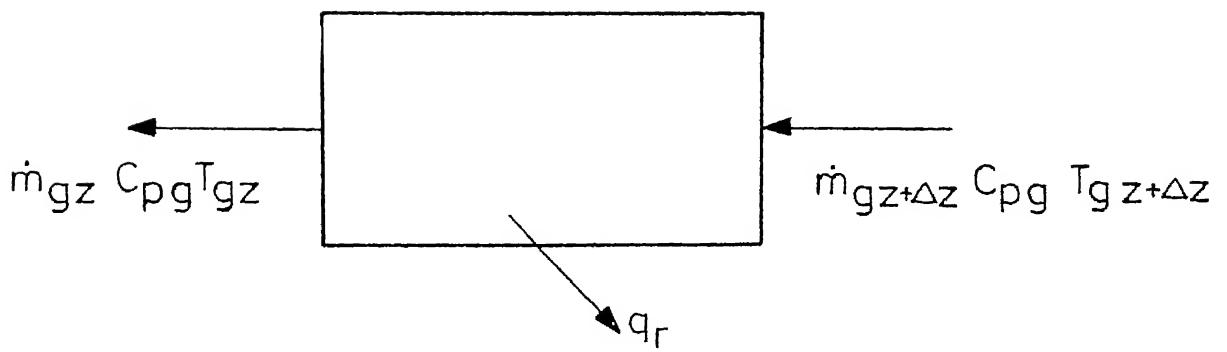

FIG.8 ENERGY BALANCE OF HOT GAS IN THE 1^{st} AND 3^{rd} SECTIONS

where q_r is the total heat lost from the hot gas due to radiation. But the heat lost by the gas is gained by wall surface and solid surface. So

$$q_r = \sum_{j=1}^{20} q_j \tag{2.14}$$

where q_j is same as given in equation (2.1). Since there is no change in mass flow, $\dot{m}_{g.Z} = \dot{m}_{g.Z+\Delta Z}$. Thus from equation (2.13), it can be written as

$$T_{g.Z+\Delta Z} = T_{g.Z} + \frac{q_r}{\dot{m}_{g.Z}\, C_{pg}} \tag{2.15}$$

In the second region, due to evaporation, rate of flow is also changing. Fig. 9 shows the mass balance of gas in the second section. Referring this figure it can be written as

$$\dot{m}_{g.Z+\Delta Z} = \dot{m}_{g.Z} - \dot{m}_V \tag{2.16}$$

Again, in the second section, superheating of vapour also takes place over and above the heating of wall surface and solid. Fig. 10 shows the energy balance of gas in the second section. If C_V is the specific heat of vapour, it can be written as

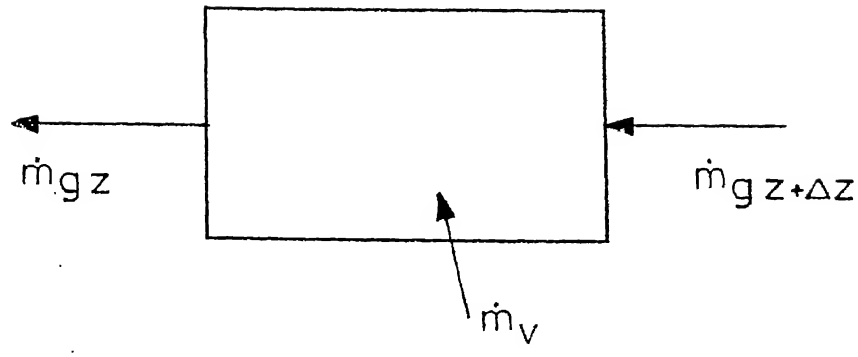

FIG.9 MASS BALANCE OF GAS IN THE SECOND SECTION

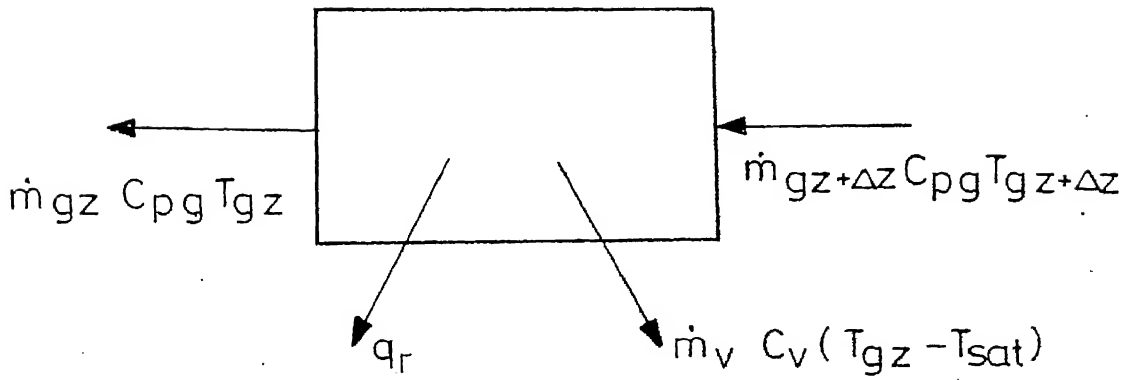

FIG.10 ENERGY BALANCE OF THE GAS IN THE SECOND SECTION

$$\dot{m}_{g.Z+\Delta Z}\, C_{pg}\, T_{g.Z+\Delta Z} = \dot{m}_{g.Z}\, C_{pg}\, T_{g.Z} + q_r + \dot{m}_V\, C_V\, (T_{g.Z}-T_{sat})$$

or

$$T_{g.Z+\Delta Z} = \frac{\dot{m}_{g.Z}}{(\dot{m}_{g.Z} - \dot{m}_V)}\, T_{g.Z} + \frac{q_r + \dot{m}_V C_V (T_{g.Z}-T_{sat})}{(\dot{m}_{g.Z} - \dot{m}_V)\, C_{pg}} \qquad (2.17)$$

Thus the temperature of gas in the next segment can be calculated.

It should be noted that the temperature of the gas and the solid in each axial segment have been taken as uniform in this analysis.

Chapter 3

Method of Solution

A computer program is developed to obtain a numerical solution to the heat transfer equations. For solving the heat transfer problem, the kiln is divided into segments of equal length, ΔZ, in the axial direction. In this problem ΔZ is taken as 1.0 m. Also, the fill angle, α, is taken to be 90^{o} (which is same as that of Sass's kiln). The solid temperature and mass flow rate are known at the inlet of the kiln. The outlet gas temperature at the inlet of the kiln, since the flow is countercurrent, is also assumed to be known and also the rate of flow. The percentage of liquid in the incoming wet solid is also known.

Thus the heat transfer equations can be solved at the first segment in the preheating zone. The temperature of solid leaving the first segment is calculated using equation (2.7). The temperature of gas in the second segment is also calculated using equation (2.15). Now the second segment can be analysed and it is proceeded similarly.

Once the wet solid temperature reaches the boiling temperature of the entrained liquid, evaporation starts.

In this section, the mass flow rate of both solid and gas and the temperature of gas in the next segment are calculated using equations (2.8), (2.16) and (2.17), respectively. The temperature of solid remains constant in this section.

Once the whole quantity of liquid is evaporated, the post heating starts. Here also similar to first section, equations (2.7) and (2.15) are used for calculating the temperatures of solid and gas respectively, in the next segments.

Once the temperature of solid reaches the required value, the computation stops and hence the length of the kiln required to dry the wet solid and preheat to a desired temperature can be calculated.

Figure 11 shows a concise flow chart of the computer program developed to solve the problem. The parameters and their values that have been given as input to the program are listed in Table 1. A copy of the computer program is listed in Appendix D.

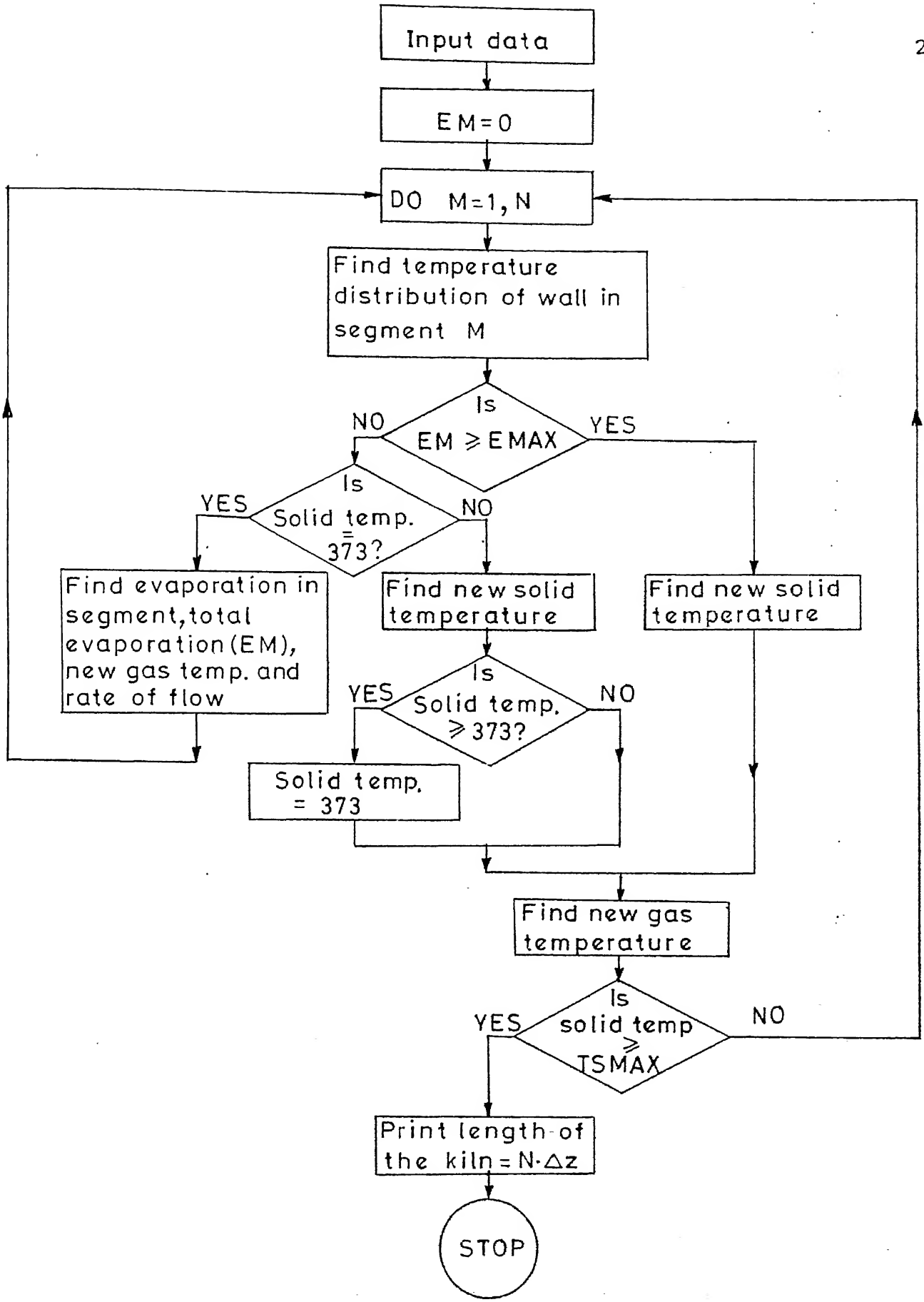

FIG·11 FLOW CHART OF THE PROGRAM

Table 1. Input Data to Program

I. Rotary Kiln		
A. Diameter	:	1.95 m
B. Refractory		
1. Thickness	:	0.3 m
2. Thermal conductivity	:	1.3274 $W/m^{\circ}K$
3. Specific heat	:	692.556 $J/kg.^{\circ}K$
4. Density	:	3000 kg/m^3
5. Emissivity	:	0.9
II. Solid		
A. Inlet temperature	:	366.66 $^{\circ}K$
B. Mass flow rate (dry)	:	2.996 kg/sec.
C. Specific heat	:	1122.54 $J/kg.^{\circ}K$
D. Water in solid feed	:	18% (by weight)
E. Emissivity	:	0.95
III. Gas		
A. Outlet temperature	:	935.77 $^{\circ}K$
B. Specific heat	:	1214.7 $J/kg.^{\circ}K$
C. Mass flow rate	:	5.9075 kg/sec,
D. Transmissivity	:	0.5
IV. Liquid-Water		
A. Latent heat of vaporisation	:	2.26×10^6 J/kg
B. Specific heat (vapour)	:	2083.2 $J/kg.^{\circ}K$

V. Heat Transfer Coefficient

A. Solid and refractory surface : 64 $W/m^2.{}^oK$

B. Outer wall and surrounding (only by convection) : 10 W/m^2-K

VI. Fill Angle : 90^o.

Chapter 4

Results and Discussion

As has been mentioned earlier in the first chapter, the main objective of this work is the development of a kiln model which is more rigorous and improved than the simplified model of Sass [1]. Sass did not consider the circumferential variation of temperature in the refractory wall and his study is based mostly on various heat transfer correlations in contrast with the present work.

The accuracy of the kiln simulation has been tested by comparing the present computer solution against that of Sass [1] and the actual kiln operating data. The set of data is obtained for a cement kiln from Sass [1] and is the only set of complete kiln temperature-profile data available in literature.

The cement kiln temperature-profile data were obtained as part of a detailed analysis of cement kiln operation. The kiln was actually 185 ft. long, but since the present simulation neglects chemical reaction, only the 89.5 ft. portion of the kiln in which no chemical reaction occurs was used for comparison with the computer results.

Figure 12 shows a comparison of temperature-profiles of the solid and the gas as a function of percent kiln length with those predicted by Sass [1] and with the actual measured data. Although some of the predicted temperatures are slightly low as compared to the other two, it is apparent that the simulation has accurately predicted the gas-temperature profile in the kiln, the fraction of the kiln used for water evaporation and the fraction used for heating the solids.

However, the kiln length as predicted by the present model turns out to be 64 ft. as compared with 83.5 ft. as predicted by Sass [1] and 89.5 ft. which is the length of the actual kiln.

The possible causes of deviation of the predicted results of the present work from those of Sass [1] and experimental data are the uncertainity in the input data to the computer program - for example.

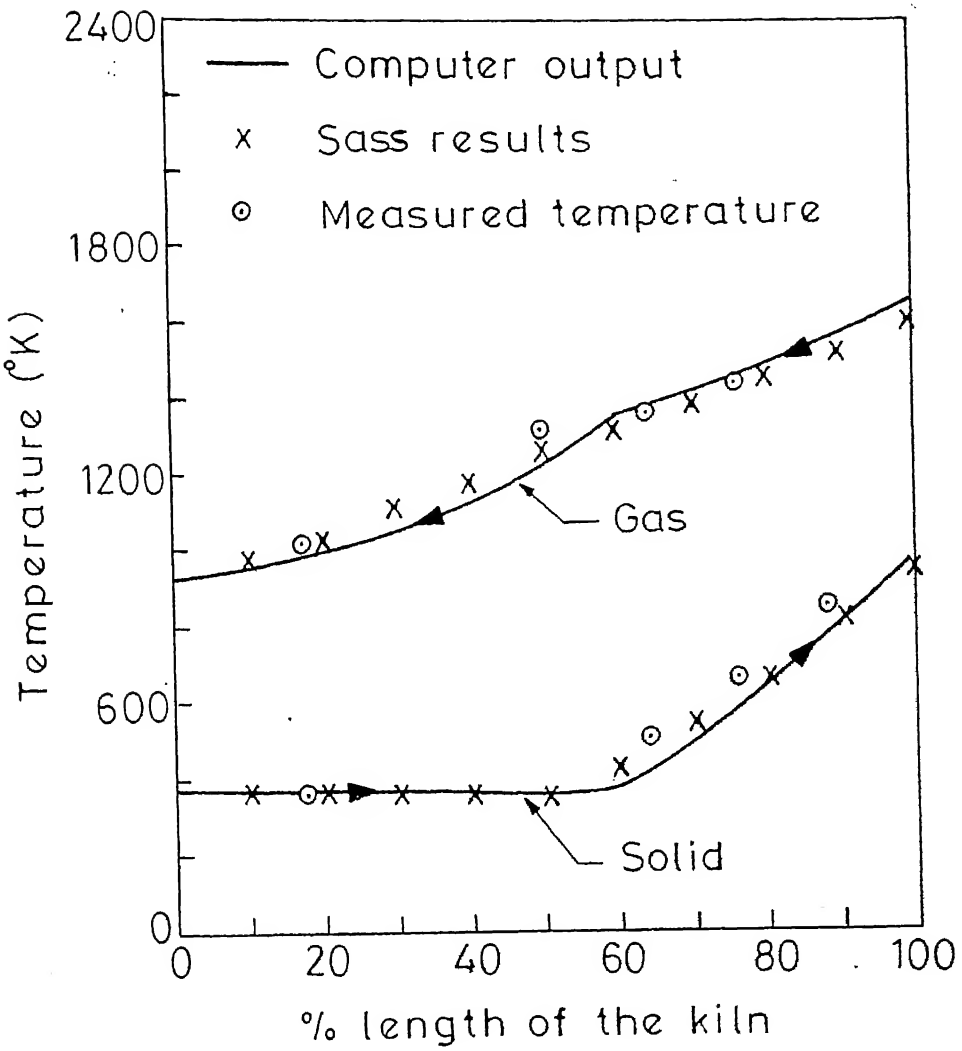

FIG-12 AXIAL TEMPERATURE DISTRIBUTION OF SOLID AND GAS

(i) In Sass's paper no mention is made about the gas composition. The gas composition used in this work has been taken from a cement kiln hand book. Actually, the gas used in the kiln might be having different composition.

(ii) The fill-angle of 90° used here has been indirectly calculated from the data given by Sass. Sass has not explicitly indicated the actual fill-angle.

(iii) Actual heat transfer coefficient from the inner wall of the kiln to the solid is not known. Only an estimate has been used.

(iv) The actual ambient temperature outside the kiln is not stated in Sass's paper. Also, the actual heat transfer coefficient from the outside of the kiln to the surroundings is not known. Here also, an estimate has been used.

(v) No measurement of the solid-exit temperature or the gas-inlet temperatures are available. The values used are based on estimates made by operating personnel.

Figure 13 shows the circumferential temperature variation of the inner kiln wall in the first axial segment of the kiln. The minimum temperature occurs at a point ($\theta \approx 90^{\circ}$) where the wall emerges from the solid. After the wall comes out of the solid, it experiences a rise in temperature because it is then exposed to radiation

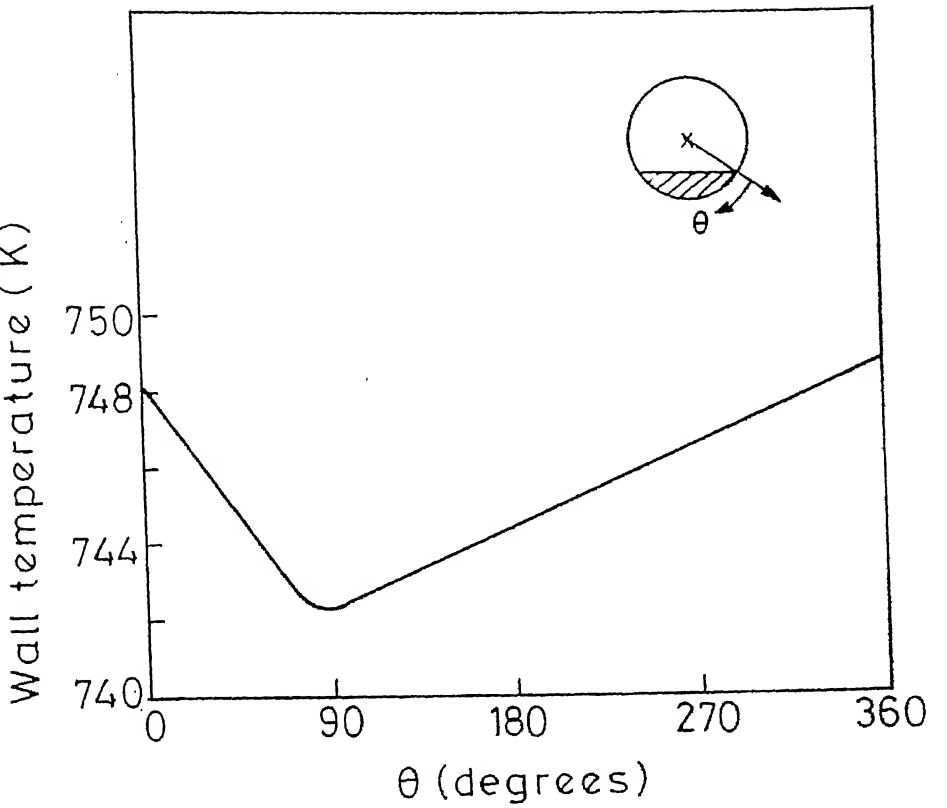

FIG.13 THE CIRCUMFERENTIAL TEMPERATURE DISTRIBUTION OF THE INNER KILN WALL IN THE FIRST AXIAL SEGMENT OF THE KILN

from the hot gas. The temperature rise continues until it is again covered by the solid ($\theta = 360^{o}$ or 0^{o}). However, it is clearly evident from the graph that the difference between the minimum temperature (742 ^{o}K) and the maximum temperature (748^{o}K) is very small - which justifies the assumption by Sass that there is no circumferential temperature variation in the kiln wall.

Figure 14 shows the radial temperature distribution of the kiln wall in the first axial segment of the kiln. It is clear that the temperature profile is almost linear.

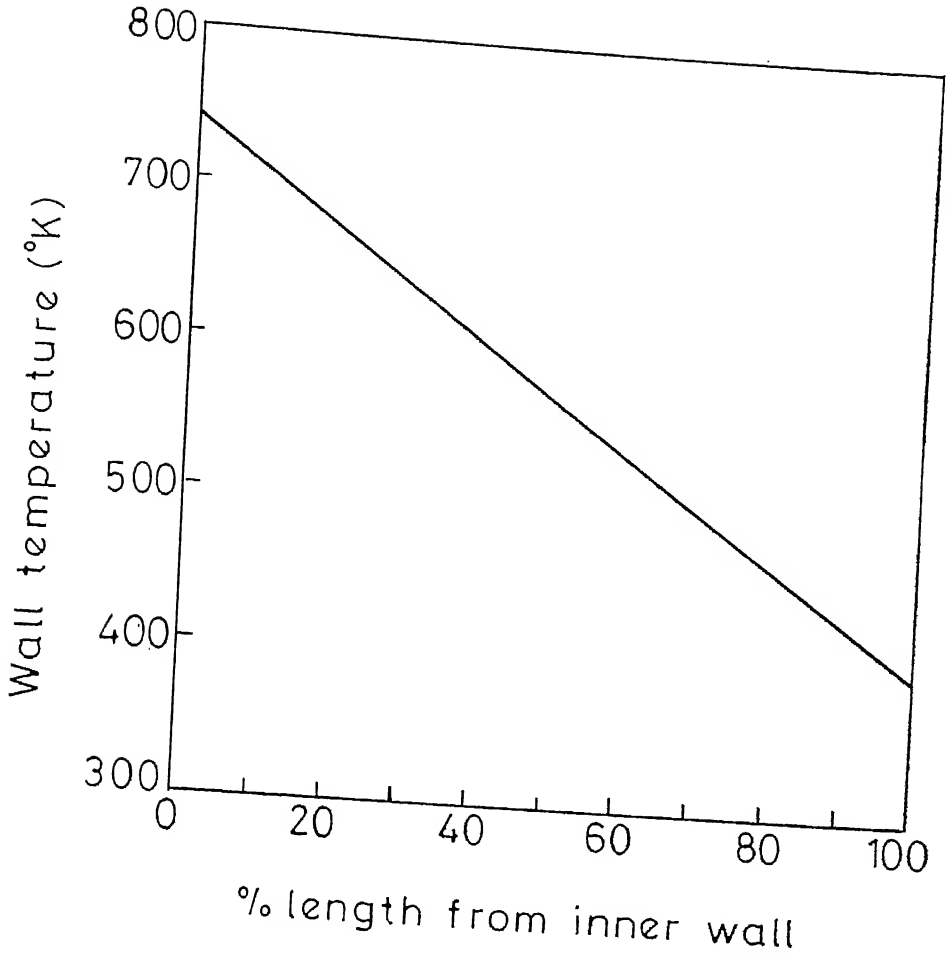

FIG·14 THE RADIAL TEMPERATURE DISTRIBUTION OF THE KILN WALL IN THE FIRST AXIAL SEGMENT

Chapter 5

Conclusion and Recommendation

The present model developed for the non-reacting zone of a cement rotary kiln is an improvement over Sass's model and can be used to design an actual rotary kiln used for drying and preheating of wet solids in many industries. Although the length of the kiln predicted by the present model shows a much lower value than that of the actual kiln, the axial gas and solid temperature distribution Vs. percent length of kiln matches well with the actual kiln profile. The main reason why the predicted kiln length doesn't match is the uncertainity in some of the input data. This can be overcome by checking the results of the theoretical model with a companion laboratory scale experimental set-up. For example, heat transfer coefficient from the wall to the solid, h_{cs}, should be calculated from the data of an actual experimental work. Same can be said of the heat transfer coefficient from the outside kiln wall to the ambient. Lastly, future efforts should be made in the direction of the design of an entire cement kiln which includes the reacting zone as well.

Chapter 6

References

1. Sass Allan, "Simulation of the heat transfer phenomenon in a rotary kiln", Ind. Eng. Chem. Process Design and Development, Vol. 6, No. 4, Oct. 1967, pp. 532-535.

2. Manitius, Andrezej, Kureyuz Ewa, and Kawecki Weislaw, "Mathematical model of the Aluminium oxide rotary kiln", Ind. Eng. Chem. Process Design and Development", Vol. 13, No. 2,1974, pp. 132-142.

3. Mason, L. and Unger, S., "Hazardous Material Incinerator Design Criteria", EPA Report No. 600/2-79-198, Oct.1979.

4. Ghoshdastidar, P.S., Rhodes, C.A., and Orloff, D.I., "Heat Transfer in a Rotary Kiln during Incineration of Solid Waste", Presented at the 23rd National ASME/AIChE Heat Transfer Conference in Denver, Colrado, USA, August 1985. ASME Paper No. 85-HT-86.

5. Ing. Paul Weber, "Heat Transfer in Rotary Kilns", Bauverlag Gmbh, Wiesbaden-Berlin.

6. Holman, J.P., Heat Transfer, 4th ed. McGraw Hill Kogakusha Ltd., Tokyo.

7. Helmrich Harold and Shugerl Karl, "Rotary Kiln Reactors in Chemical Industry", Ger. Chem. Engg. 3 (1980), pp. 194-202.

8. Suryanarayana, N.V., Lyon, J.E., and Kim, N.K., "Heat Shield for High Temperature Kiln", Ind. Eng. Chem. Process Design and Development, 1986, 25, pp. 843-849.

9. Jacob, Max, Heat Transfer, Vol. II, 1st ed., John Wiley & Sons, Inc., New York, pp. 19-21.

Appendix A

A.0 Calculation of Shape Factors

The shape factors between the fifteen refractory surface elements and five solid surface elements are determined assuming the surfaces as infinite parallel strips. The equation for shape factors for infinite parallel strips was derived by Hottel [9]. Surfaces (1) and (2) in Fig. A.1 are strips perpendicular to the XY plane and is measured from the normal to the surface (1). The shape factor F_{1-2} is given by

$$F_{1-2} = \frac{\text{Sin } \phi' - \text{Sin } \phi''}{2} \qquad \text{(A.1)}$$

A detailed analysis of this shape factor calculation was done by Ghoshdastidar et al [4].

A.1 Shape Factors between the Elements of the Kiln Wall

Equation (A.1) is written in terms of the circumferential location of the two surfaces. For the notation shown in Fig. A.2, the shape factor between surface (1) and (2) is given by

$$F_{1-2} = \frac{\Delta\theta \cdot \text{Cos}\beta}{4} \qquad \text{(A.2)}$$

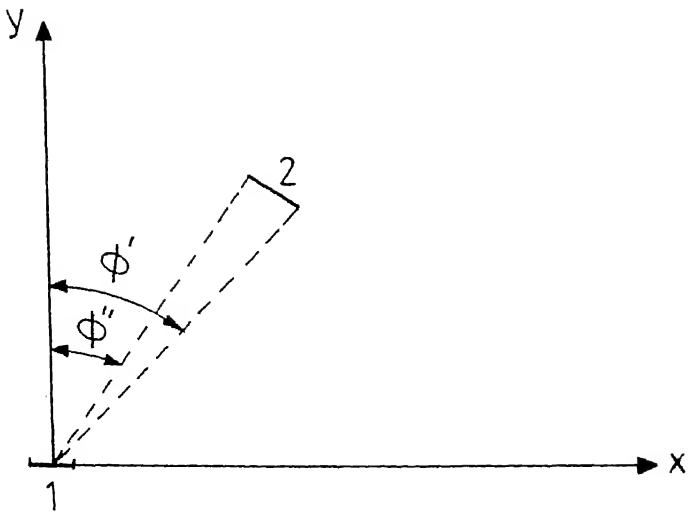

FIG. A-1 SHAPE FACTOR BETWEEN INFINITE PARELLEL SURFACES

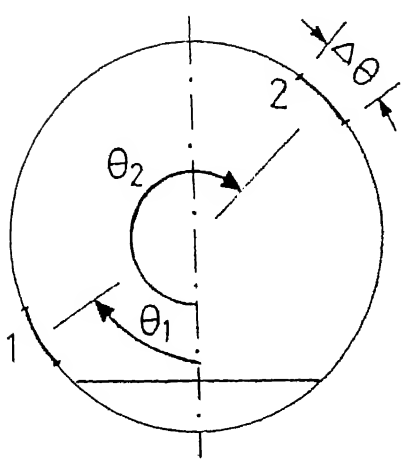

FIG. A-2 SHAPE FACTOR NOMENCLATURE WHEN BOTH SURFACES ARE ON THE REFRACTORY WALL

where $\Delta\Theta$ is the arc angle of surface (2) in radian. The angle β is defined as

$$\beta = \frac{\pi - |(\Theta_2 - \Theta_1)|}{2} \qquad (A.3)$$

where Θ_1 and Θ_2 are the circumferential position of surface elements (1) and (2) respectively with respect to the reference axis. For convenience, the reference axis is chosen perpendicular to the solid surface. Because of the absolute bracket in equation (A.3), the shape factors F_{1-2} and F_{2-1} are equal for the same $\Delta\Theta$ as required by the reciprocity relations of shape factors.

A.2 Shape Factors between Elements of the Kiln Wall and Solid Surface

In Fig. A.3, surface (1) is a solid surface element and surface (2) is a refractory wall element. Surface (1) is located at a distance b from the reference axis and Θ_2 is the circumferential angle for surface (2). Angle α is the fill angle of the solid material. Additional terms which are shown in Fig. A.4 are needed to determine the shape factor. The shape factor F_{1-2} is given by

$$F_{1-2} = \frac{D \cos \Psi_1 \cos \Psi_2 \Delta\Theta}{4e} \qquad (A.4)$$

where D is the inside diameter of the kiln. The angle

Ψ_1 and Ψ_2 are shown in Fig. A.3 and are respectively the angles between the normals to surface (1) and (2) and the ray extending between the surfaces. The distance e is the length of this ray. Expressions for Ψ_1, Ψ_2 and e in terms of parameters shown in Fig. A-4 were derived by Ghoshdastidar [4] and are as follows:

$$\Psi_3 = \tan^{-1} (2b/D \cos \alpha/2) \qquad \text{(A.5a)}$$

$$C = (D \cos \alpha/2)/2 \cos \Psi_3 \qquad \text{(A.5b)}$$

$$e = [C^2 + D^2/4 - C D \cos (2\pi - \theta_2 + \Psi_3)]^{1/2} \qquad \text{(A.5c)}$$

$$\Psi_2 = \sin^{-1} [C \sin(2\pi - \theta_2 + \Psi_3)/e] \qquad \text{(A.5d)}$$

$$\Psi_1 = \theta_2 - \Psi_2 - \pi \qquad \text{(A.5e)}$$

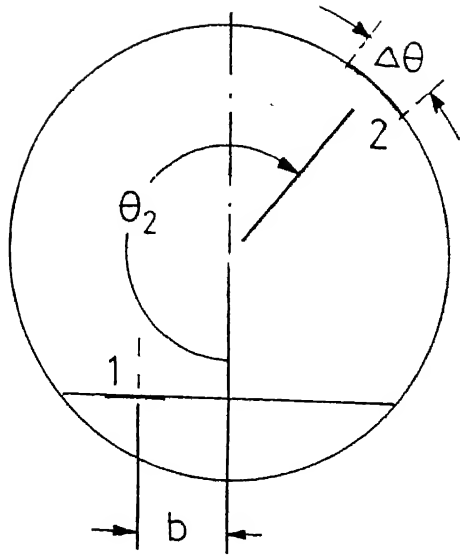

FIG. A-3 SHAPE FACTORS NOMENCLATURE WHEN ONE SURFACE IS ON REFRACTORY AND THE OTHER IS ON SOLID

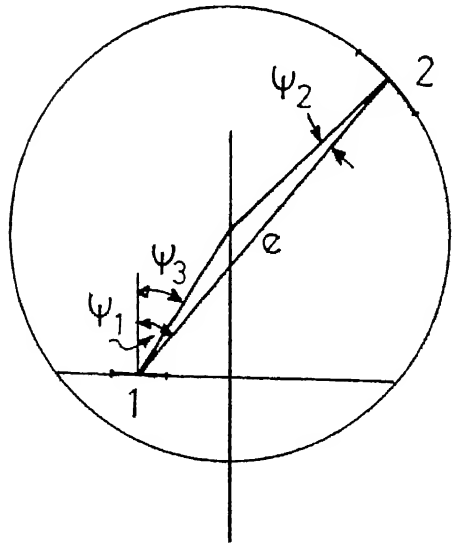

FIG. A-4 PARAMETERS FOR SHAPE FACTOR EQUATION

Appendix B

Calculation of the Emissivity of the Gas

For the calculation of the emissivity of the hot gas, we require the composition of the gas. Of the gases encountered in heat transfer equipments, carbon monoxide, the hydrocarbons, water vapour, carbon dioxide, sulpher dioxide, ammonia, hydrogen chloride and the alcohols are among those with emission bands of sufficient magnitude to merit consideration. Gases with symmetrical molecules, hydrogen, oxygen, nitrogen etc. have been found not to show absorption bands in those wavelength regions of importance in radiant heat transmission at temperatures met in industrial practice.

The composition (by volume) of hot gas for a typical cement rotary kiln was obtained from Ing. Paul Weber [5], and is as follows:

CO_2 - 15.897%

O_2 - 1.418%

N_2 - 41.784%

H_2O - 40.9%

Thus we see that only CO_2 and water vapour are the gases having any effect on emissivity. For calculation of emissivity, we are using the method suggested by Holman [6], using mean beam length, Le.

Since mean beam length information for this particular geometry is not available, as per Holman [6], we can use the following approximation

$$Le = 3.6 \frac{V}{A} \qquad (B.1)$$

where V is the total volume of the gas and A is the total surface area. For the fill angle of $\alpha = 90^{o}$ in the present work, we can see that

$$Le = 3.6 \left| \frac{\frac{3}{4}\pi R^2 + \frac{1}{2} R^2}{\frac{3}{2}\pi R + \sqrt{2}\ R} \right|$$

i.e. $Le = 1.6783\ R.$

where R is the internal radius.

If the pressure inside the kiln is assumed to be 1 atmosphere, then partial pressure of CO_2 and water vapour can be obtained as 0.1589 atm. and 0.409 atm. respectively. Radius of the kiln is 3.25 feet.

Using the above values and the method given in [6] and converting the temperature scale into degree Kelvin, we can tabulate the emissivities as in Table 2.

Table 2. Emissivity of Hot Gas at Different Temperature Ranges

Temperature range ^{o}K		Emissivity
From	To	
273.0	347.0	0.6304
347.0	486.0	0.5524
486.0	625.0	0.5358
625.0	764.0	0.5408
764.0	903.0	0.5210
903.0	1042.0	0.5028
1042.0	1181.0	0.4680
1181.0	1320.0	0.4170
1320.0	1459.0	0.3838
1459.0	1598.0	0.3506
1598.0	1737.0	0.3202

Appendix C

C.0 Finite Difference Scheme

A. Inside Surface Exposed to Radiation from the Hot Gas

Refer Fig. C-1. Here q is the radiation heat input into the element on the refractory walls from the hot gas. As per the coordinate system already explained, we can see that

$$\Delta Y = R \left(\frac{2\pi - \alpha}{15}\right)$$

where α is the fill angle in radian

$$\Delta X = \left(\frac{\text{Thickness}}{10}\right) = \frac{0.3}{10} = 0.03 \text{ m}$$

Then finite difference equation can be written as

$$-K\ \Delta Y.\Delta Z\ \frac{T^{p}_{m,n} - T^{p}_{m+1,n}}{\Delta X} + q = \rho_s\ C\ \frac{\Delta X}{2}\ \Delta Y\ \Delta Z\ \frac{T^{p+1}_{m,n} - T^{p}_{m,n}}{\Delta \tau}$$

$$+ \rho_s\ C\ \frac{\Delta X}{2}\ \Delta Y\ \Delta Z.\ U.\ \frac{T^{p}_{m,n} - T^{p}_{m,n-1}}{\Delta Y} \qquad (C.1)$$

B. Inside Surface Covered by Solid

Refer Fig. C.2. Here, the area covered by the solid is divided into five elements. So

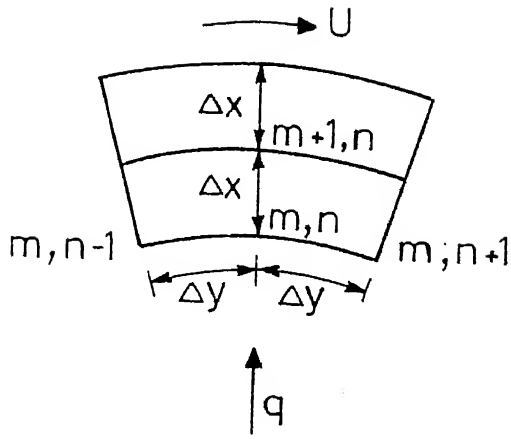

FIG. C-1

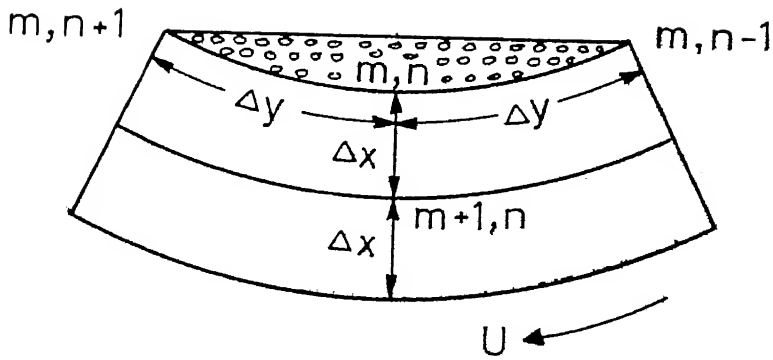

FIG. C-2

$$\Delta Y = R \cdot \frac{\alpha}{5}$$

$$\Delta X = 0.03 \text{ m.}$$

In this case, the finite difference equation can be written as follows:

$$-K.\Delta Y\Delta Z \cdot \frac{T^p_{m,n} - T^p_{m+1,n}}{\Delta X} = \rho_s C \frac{\Delta X}{2}\Delta Y.\Delta Z \frac{T^{p+1}_{m,n} - T^p_{m,n}}{\Delta \tau}$$

$$+ h_{cs}(T^p_{m,n} - T_s)\Delta Y.\Delta Z + \rho_s C \frac{\Delta X}{2} .\Delta Y.\Delta Z. U \frac{T^p_{m,n} - T^p_{m,n-1}}{\Delta Y} \qquad (C-2)$$

C. Interior Point

Refer Fig. C-3, For a general interior point, ΔY can be calculated as

$$\Delta Y = [R + (K-1)\ \Delta X] \frac{2\pi - \alpha}{15}$$

where K is the grid number in X direction and

$$\Delta X = \frac{\text{Thickness}}{10} = 0.03 \text{ m.}$$

Then finite difference equation can be written as follows:

$$\frac{T^p_{m+1,n} + T^p_{m-1,n} - 2T^p_{m,n}}{(\Delta X)^2} = \frac{1}{a_{rf}} \frac{T^{p+1}_{m,n} - T^p_{m,n}}{\Delta\tau}$$

$$+ \frac{U}{a_{rf}} \frac{T^p_{m,n} - T^p_{m,n-1}}{\Delta Y} \qquad (C.3)$$

where a_{rf} is the thermal diffusivity of the refractory material.

D. Outer Surface Exposed to Ambient Air

Refer Fig. C.4. If hr is the combined radiation and convection heat transfer coefficient for the outer surface, then the finite difference equation can be written as follows:

$$-K.\Delta Y\Delta Z \frac{(T^p_{m-1,n} - T^p_{m,n}}{\Delta X} = \rho_s C. \frac{\Delta X}{2} .\Delta Y.\Delta Z \frac{T^{p+1}_{m,n} - T^p_{m,n}}{\Delta\tau}$$

$$+ h_r (T^p_{m,n} - T_{inf})\Delta Y.\Delta Z + \rho_s C. \frac{\Delta X}{2} .\Delta Y.\Delta Z. U. \frac{T^p_{m,n} - T^p_{m,n-1}}{\Delta Y}$$

where T_{inf} is the ambient temperature in degree Kelvin.

In the above cases, the circumferential velocity, U, is calculated using the formula, $U = \frac{\pi DS}{60}$ where S is the number of revolution per minute of the kiln.

C.1 Method of Solution

Equations (C.1), (C.2), (C.3) and (C.4) are solved simultaneously at each time step $\Delta\tau$ using explicit

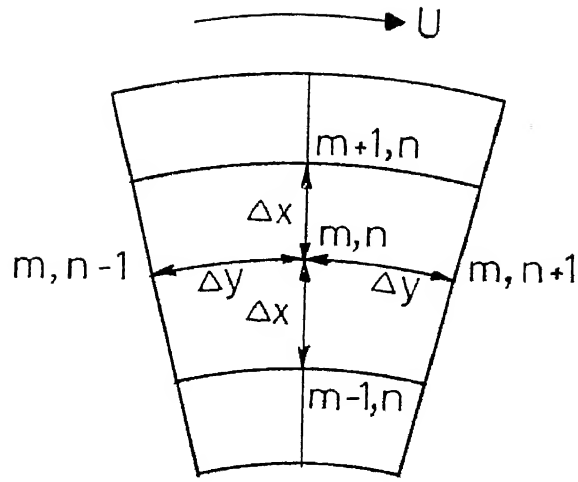

FIG. C-3

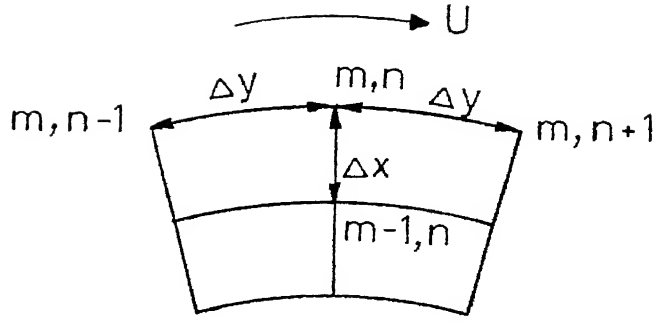

FIG. C-4

method. A time step of $\Delta\tau = 1$ second was taken. Since the initial temperature distribution of the refractory wall was not known, an arbitrary temperature was assumed at all grid points in the refractory wall. The solution converges when there is no further change in the temperatures at each grid point as $\tau \to \infty$. This temperature distribution represents the steady state temperature distribution of the wall.

```
C ***********************************************************************
C
C       PROGRAM FOR SIMULATION OF HEAT TRANSFER IN CEMENT ROTARY KILN
C
C ***********************************************************************
C
        DIMENSION F(20,20),TH(20),TT4(20),B(5),FS(20)
        DIMENSION QR(20),A(20),FG(20),TEMP(20),TEMPT(22,11),QC(5)
        DIMENSION TSW(200),TEMPG(200)
        OPEN(UNIT=25,DEVICE='DSK',FILE='FOR25.DAT')
        OPEN(UNIT=26,DEVICE='DSK',FILE='FOR26.DAT')
C ***********************************************************************
C       DEFINITION OF TERMS USED
C ***********************************************************************
        D - - - - Inner diameter of the Kiln (M)
        ALPHA - - Fill angle of the solid (Radians)
        TEMPG - - Temperature of the gas (Degree K)
        DELT  - - Time interval in seconds
        SIGMA - - Stefen Boltzman constant
        RO  - - - Density of refractory KG/CU.M
        CPR - - - Specific heat of refractory (J/KG.K)
        CPS - - - Specific heat of solid (J/KG.K)
        CPG - - - Specific heat of gas (J/KG.K)
        HCS - - - Convective heat transfer coeff(inside) (W/Sq M.K)
        HRS - - - Combined heat transfer coeff.(Outside) (W/Sq M.K)
        TSW - - - Temperature of solid (Degree K)
        TINF  - - Ambient temperature (Degree K)
        PK- - - - Conductivity of refractory (W/M.K)
        THICK - - Thickness of refractory wall (M)
        U - - - - Circumferential velocity of solid (M/Sec)
        TOWG  - - Transmissivity of gas
        EPSG  - - Emissivity of gas
        SMASS - - Mass flow rate of dry solid (KG/Sec)
        GMASS - - Masslw rate of hot gas (KG/Sec)
        EMAX  - - Quantity of water tobe evaporated (KG/Sec)
        HLAT - - Latent heat of vaporisation of water (J/KG)
        HLOSS - - Total heat loss from outer surface (W)
        QR  - - - Radiation heat transfer (W)
        QC  - - - Convection heat transfer (W)
        TEMPT - - Temperature of wall (Degree K)
        F(I,J)- - Shape factor
C ***********************************************************************
        D=1.95
        TEMPG(1)=935.77
        DZ=1.0
        TSW(1)=366.66
        TSMAX=977.4
        CPG=1214.7
        GMASS=5.0075
```

```
      SMASS=2.9963
      EMAX=0.5393
      SIGMA=5.669E-8
      RO=3000.0
      CPR=692.556
      HC=10.0
      HCS=64.0
      THICK=0.3
      U=-0.1908
      DELP=1.
      TOWS=0.5
      HILAT=2.26E+6
      CPV=2083.2
      CPS=1122.54
      PI=3.1415926
      ALPHA=PI/2.
      DELTH=(2.*PI-ALPHA)/15.
      R=D/2.
C *****************************************
C     CALCULATION OF SHAPE FACTOR
C *****************************************
      B(1)=-8.*R*SIN(ALPHA/2.)/10.
      B(2)=B(1)/2.
      B(3)=0.
      B(4)=-1.*B(2)
      B(5)=-1.*B(1)
      DO 666 I=1,20
      L=I
      IF(I.GE.6) GO TO 111
      TH(I)=(2.*L-1.)*ALPHA/10.
      GO TO 112
111   TH(I)=ALPHA+(2.*(L-5)-1.)*DELTH/2.
112   CONTINUE
      TTH(I)=TH(I)-ALPHA/2.
666   CONTINUE
      DO 777 I=1,20
      DO 888 J=1,20
      IF (I.GE.6) GO TO 1111
      IF (J.GE.6) GO TO 1112
      F(I,J)=0.0
      F(J,I)=0.0
      GO TO 888
1112  PSI3=ATAN(2.*B(I)/(D*COS(ALPHA/2.)))
      C=D*COS(ALPHA/2.)/(2.*COS(PSI3))
      E=SQRT(C*C+D*D/4.-C*D*COS(2.*PI-TTH(J)+PSI3))
      PSI2=ASIN(C*SIN(2.*PI-TTH(J)+PSI3)/E)
      PSI1=TTH(J)-PSI2-PI
      F(I,J)=D*COS(PSI1)*COS(PSI2)*DELTH/(1.*E)
      F(J,I)=0.4*SIN(ALPHA/2.)*F(I,J)/DELTH
      GO TO 888
1111  IF(J.LE.5) GO TO 888
```

```
      BETA=ABS((ABS(ITH(I)-ITH(J))-PI)/2.)
      F(I,J)=DELTH*COS(BETA)/4.
888   CONTINUE
777   CONTINUE
C -----------------------------------------
C     VERIFICATION OF SHAPE FACTORS
C -----------------------------------------
      DO 2222 I=1,20
      FS(I)=0.0
      DO 2221 J=1,20
      FS(I)=FS(I)+F(I,J)
2221  CONTINUE
2222  CONTINUE
C *****************************************
C     WRITE(25,999)((F(I,J),I=1,20),J=1,20)
C999  FORMAT((20(F6.3))/)
C     WRITE(25,998)(FS(I),I=1,20)
C998  FORMAT((10X,F8.5)/)
      DO 213 I=1,20
      IF(I.LE.5) GOTO 214
      A(I)=R*DZ*DELTH
      GOTO 213
214   A(I)=0.4*R*DZ*SIN(ALPHA/2.)
213   CONTINUE
      AG=6.1266*R*DZ
      TINF=300.
      PK=1.3274
      DX=THICK/10.
      DO 215 I=1,20
215   FG(I)=A(I)/AG
C -----------------------------------------------------
C     INITIAL ASSUMPTION OF WALL GRID TEMP. (Degree K)
C -----------------------------------------------------
      READ(47,696)((TEMPT(I,J),J=1,11),I=1,20)
696   FORMAT((15X,11(2X,F8.3))/)
      EM=0.0
      HLOSS=0.0
      DO 100 M=1,30
      WRITE(26,992)(M,TSW(M),TEMPG(1))
992   FORMAT(10X,I3,5X,F9.3,5X,F9.3)
      DO 300 N=1,3000
C -----------------------------------------------------------------
C     CALCULATION OF WALL TEMP. USING FINITE DIFFERENCE METHOD
C -----------------------------------------------------------------
      TDEL=0.0
      DO 301 J=1,11
      DO 302 I=1,20
      IF (J.NE.1) GOTO 375
      DO 211 K=1,5
211   TEMP(K)=TSW(M)
      DO 212 K=6,20
```

```
212       TEMP(K)=TEMPT(K,1)
C  ***********************************************
C         CALCULATION OF RADIATION HEAT TRANSFER
C  ***********************************************
          IF (TEMPG(M).LE.374.) GOTO 510
          IF (TEMPG(M).LE.468.) GOTO 511
          IF (TEMPG(M).LE.625.) GOTO 512
          IF (TEMPG(M).LE.764.) GOTO 513
          IF (TEMPG(M).LE.903.) GOTO 514
          IF (TEMPG(M).LE.1042.) GOTO 515
          IF (TEMPG(M).LE.1181.) GOTO 516
          IF (TEMPG(M).LE.1320.) GOTO 517
          IF (TEMPG(M).LE.1459.) GOTO 518
          IF (TEMPG(M).LE.1598.) GOTO 519
          IF (TEMPG(M).GT.1598.) GOTO 520
510       EPSG=0.6304
          GOTO 521
511       EPSG=0.5524
          GOTO 521
512       EPSG=0.5358
          GOTO 521
513       EPSG=0.5408
          GOTO 521
514       EPSG=0.5210
          GOTO 521
515       EPSG=0.5028
          GOTO 521
516       EPSG=0.4680
          GOTO 521
517       EPSG=0.4170
          GOTO 521
518       EPSG=0.3838
          GOTO 521
519       EPSG=0.3536
          GOTO 521
520       EPSG=0.3202
521       CONTINUE
          PP=AG*FG(I)*EPSG*SIGMA*(TEMPG(M)**4)
          AKK=0.0
          DO 217 L=1,20
          AKK=AKK+A(L)*F(L,I)*TONG*SIGMA*(TEMP(L)**4)
217       CONTINUE
          EBAI=A(I)*SIGMA*(TEMP(I)**4)
          QR(I)=PP+AKK-EBAI
C  ***********************************************
375       CONTINUE
C         WRITE(25,997)(QR(I),I=1,20)
C997      FORMAT((20X,F15.4)/)
          TEMPT(21,J)=TEMPT(1,J)
          DY=(R+(J-1)*DX)*DELTH
          TNEW=0.0
```

```
      Z1=(U*DELT)/DY
      Z2=(2.*PK*DELT)/(RO*CPR*DX*DX)
      IF(J.NE.1) GOTO 376
      IF(I.EQ.1) GOTO 377
      IF (I.LE.5) GOTO 378
C -------------------------------------
CC    GRID POINTS ON THE INNER WALL
C -------------------------------------
      Z3=(2.*DELT)/(RO*CPR*DX*DY*DZ)
      TT2=TEMPT(I,1)*(1.+Z1-Z2)
      TNEW=TT2+Z2*TEMPT(I,2)-Z1*TEMPT(I-1,1)+Z3*QR(I)*0.95
      GOTO 390
378   Z4=(2.*DELT*HCS)/(RO*CPR*DX)
      TT3=TEMPT(I,1)*(1.+Z1-Z2-Z4)
      TNEW=TT3+Z2*TEMPT(I,2)-Z1*TEMPT(I-1,1)+Z4*TSW(M)
      GOTO 390
377   Z4=(2.*DELT*HCS)/(RO*CPR*DX)
      TT4=TEMPT(1,1)*(1.+Z1-Z2-Z4)
      TNEW=TT4+Z2*TEMPT(1,2)-Z1*TEMPT(20,1)+Z4*TSW(M)
      GOTO 390
376   IF (J.EQ.11) GOTO 379
      IF (I.EQ.1) GOTO 380
C -------------------------------
CC    INTERIOR GRID POINTS
C -------------------------------
      TT=(TEMPT(I,J+1)+TEMPT(I,J-1))*Z2/2.
      TNEW=TEMPT(I,J)*(1.+Z1-Z2)+TT-Z1*TEMPT(I-1,J)
      GOTO 390
380   TT5=(TEMPT(1,J+1)+TEMPT(1,J-1))*Z2/2.
      TNEW=TEMPT(1,J)*(1.+Z1-Z2)+TT5-Z1*TEMPT(20,J)
      GOTO 390
C -------------------------------------
CC    GRID POINTS ON THE OUTER WALL
C -------------------------------------
379   HC1=(TEMPT(I,J)+TINF)*(TEMPT(I,J)**2+TINF**2)
      HRS=HC+HC1*SIGMA*0.9
      Z5=(2.*DELT*HRS)/(RO*CPR*DX)
      IF (I.EQ.1) GOTO 381
      TT6=TEMPT(I,11)*(1.+Z1-Z2-Z5)
      TNEW=TT6+Z2*TEMPT(I,10)-Z1*TEMPT(I-1,11)+Z5*TINF
      GOTO 390
381   TT7=TEMPT(1,11)*(1.+Z1-Z2-Z5)
      TNEW=TT7+Z2*TEMPT(1,10)-Z1*TEMPT(20,11)+Z5*TINF
390   CONTINUE
306   TDEL=TDEL+ABS(TNEW-TEMPT(I,J))
      TEMPT(I,J)=TNEW
302   CONTINUE
301   CONTINUE
      IF(TDEL.LE..1) GOTO 308
300   CONTINUE
308   CONTINUE
```

```
C ------------------------------------------------------------------
      IF (M.GE.3) GOTO 409
      WRITE(25,996)((TEMPT(I,J),J=1,11),I=1,20)
996   FORMAT((15X,11(2X,F8.3)/)
CC    ------------------------------
CC    CALCULATION OF HEAT LOSS
CC    ------------------------------
409   HLOSS=HLOSS+HRS*DZ*PT*D*(TEMPT(1,11)-TINF)
CC    ------------------------------------------
CC    CONVECTION TO SOLID FROM REFRACTORY WALL
CC    ------------------------------------------
      DO 410 I=1,5
410   QC(I)=HCS*A(6)*(TEMPT(I,1)-TSW(M))
      SIGQC=0.0
      DO 411 I=1,5
      SIGQC=SIGQC+QC(I)
411   CONTINUE
CC    ---------------------------------
CC    RADIATION TO SOLID FROM GAS
CC    ---------------------------------
      SIGQR=0.0
      DO 412 I=1,5
      SIGQR=SIGQR+0.975*QR(I)
412   CONTINUE
      SIGQRT=SIGQR
CC    ----------------------------------------
CC    TOTAL RADIATION HEAT TRANSFER FROM GAS
CC    ----------------------------------------
      DO 413 I=6,20
      SIGQRT=SIGQRT+0.95*QR(I)
413   CONTINUE
CC    ------------------------------------------------------------
CC    CALCULATION OF SOLID AND GAS TEMP. IN THE NEXT SEGMENT
CC    ------------------------------------------------------------
      IF (EM.GE.EMAX) GOTO 450
      IF (TSW(M).EQ.373.) GOTO 430
      TSW(M+1)=TSW(M)+(SIGQR+SIGQC)/((GMASS+EMAX)*CPS)
      IF (TSW(M+1).LT.373.) GOTO 440
      TSW(M+1)=373.0
      GOTO 440
430   IF (EM.NE.0.0) GOTO 460
CC    ------------------------------
CC    PL1 = LENGTH OF PREHEATING ZONE
CC    ------------------------------
      M1=M-1
      PL1=M1*DZ
CC    ------------------------------------------------------
CC    DEM = AMOUNT OF WATER EVAPORATED IN THIS SEGMENT
CC    ------------------------------------------------------
460   DEM=(SIGQR+SIGQC)/HLAT
      BT=(GMASS+EMAX-EM)/(GMASS+EMAX-EM-DEM)
```

```
      EM=EM+DEM
      AMTT=SIGORT+DEM*CPV*(TEMPG(M)-373.0)
      TEMPG(M+1)=TEMPG(M)*BT+AMTT/((GMASS+EMAX-EM)*CPG)
      TSW(M+1)=373.0
      GOTO 99
440   TEMPG(M+1)=TEMPG(M)+SIGORT/((GMASS+EMAX)*CPG)
      GOTO 99
450   IF (TSW(M).EQ.373.) GOTO 480
      GOTO 490
C -----------------------------------------
CC      PL2 - LENGTH OF EVAPORATING ZONE
C -----------------------------------------
480   M2=M-1
      PL2=(M2-M1)*DZ
490   TSW(M+1)=TSW(M)+(STGOR+SIGOC)/(SMASS*CPS)
      TEMPG(M+1)=TEMPG(M)+SIGORT/(GMASS*CPG)
C -----------------------------------------
CC      PL3 - LENGTH OF POSTHEATING ZONE
C -----------------------------------------
      M3=M-M2
      PL3=M3*DZ
C -----------------------------------------
CC      PL - TOTAL LENGTH OF THE KILN
C -----------------------------------------
      PL=M*DZ
      IF (TSW(M+1).GE.TSMAX) GOTO 500
99    CONTINUE
      DO 492 I=1,20
      DO 492 J=1,11
492   TEMPT(I,J)=TEMPT(I,J)+25.
100   CONTINUE
500   WRITE(26,982)(TSW(M+1),TEMPG(M+1))
982   FORMAT(10X,F9.3,5X,F9.3)
      WRITE(26,995) (PL1,PL2,PL3,PL)
995   FORMAT((10X,1F12.3)/)
      WRITE(26,991) HLOSS
991   FORMAT(20X,F15.3)
      STOP
      END
```